PLOS ONE

RESEARCH ARTICLE

Inventory of water masses and carbonate system from Brazilian's northeast coast: Monitoring ocean acidification

Carlos Augusto Ramos e Silva[1,2,3]*, **Nicole Silva Caliman Monteiro**[1], **Luciana Miranda Cavalcante**[4], **Waldemar Tavares Junior**[4], **Maria Eulália Rocha Carneiro**[4], **Flavo Elano Soares de Souza**[5], **Carlos Alexandre Borges Garcia**[6], **Raimundo Nonato Damasceno**[3], **Anderson de Araújo Rocha**[3]

1 Postgraduate Program in Oceans and Earth Dynamics, Geosciences Institute, Federal Fluminense University, Niterói, RJ, Brazil, 2 Marine Biology Department, Biology Institute, Federal Fluminense University, Niterói, RJ, Brazil, 3 Center of Studies on Water, Biomass, and Oil—NAB, Federal Fluminense University, Niterói, RJ, Brazil, 4 Research and Development Center—Leopoldo Américo Miguez de Mello (CENPES), Ilha do Fundão, Cidade Universitária, Rio de Janeiro, RJ, Brazil, 5 Agricultural School of Jundiaí, Federal University of Rio Grande do Norte, Jundiaí District, Macaíba, Rio Grande do Norte, Brazil, 6 Chemistry Department, Federal University of Sergipe, University District Professor José Aloísio de Campos, São Cristovão, SE, Brazil

* caugusto_99@yahoo.com

Abstract

This manuscript presents an inventory of the carbonate system from the main water masses comprising the marine current system on Brazil's northeast coast (South Atlantic Ocean). For this purpose, four transects were conducted with an approximate length of 357 km (each one) through the platform and continental slope of the Sergipe–Alagoas sedimentary basin. Water samples were then collected in vertical profiles measuring from 5 to 1,799 meters depth, totaling 34 stations. Total alkalinity, calcium, and total boron were obtained analytically from these samples and by relationships with salinity. Speciation and concentration of the carbonate system were obtained by means of thermodynamic modeling. The results revealed that the empirical models used to calculate the concentrations of TA, calcium and total boron showed relevant variation when compared to the analytical values (TA: 5.0–6.5%; Ca: 0.4–4.8%; B_T: 7.0–18.9%). However, the speciation and concentration of the carbonate system (CA, DIC, CO_3^{2-}, $CO_{2(aq)}$, Ω_{Calc}, and Ω_{Arag}) obtained from the empirical values of TA, calcium and total boron did not differ significantly from those obtained analytically (0.0–6.1%). On the other hand, the parameters of pH, HCO_3^-, $CO_{3(aq)}^{2-}$, $CO_{2(aq)}$, ρCO_2, Ω_{Calc}, and Ω_{Arag} varied significantly within the different water masses (p < 0.05). This study supports and encourages acidification monitoring projects in the South Atlantic Ocean, based on modeling the carbonate system parameters generated in real-time.

Introduction

Carbon dioxide (CO_2) sources, transport mechanisms, and transformations are an important matter in oceanography field studies [1]. CO_2 can exhibit significant spatial and temporal variability within the same water mass since the ocean content is dependent on processes such as the atmospheric exchange through sea surface and the degradation of organic matter (both autochthonous and allochthonous derived) [2]. Increasing CO_2 content will lead to both reduction in both carbonate content and pH ($CO_3^{2-} + H_2O + CO_2 = 2HCO_3^-$); this process is called *ocean acidification* (OA) [3]. It is known that OA can reduce the capacity of marine organisms (*e.g.*, coccolithophorids, corals, foraminifera, and bony fishes) because of the increased concentration of H^+ ions in seawater [4]. Understanding the acidification process is necessary for predicting future climate changes and responses from marine biota [5–7].

Efforts have been made to implement coordinated monitoring programs and increase understanding of OA [8, 9]. The main actions required for the implementation of these programs consist of (1) creating a database of the carbonate system of coastal ecosystems (spatial and temporal), (2) standardization in pH and TA determinations, and (3) transparency in precision of the polynomials responsible for generating the data of the carbonate system [8–12].

An OA monitoring network requires constant maintenance of the records of the main chemical parameters, for example pH and total alkalinity, which allows the determination of the saturation state of the aragonite (Ω_{Arag}) and a complete description of the carbonate system [9]. The parameters suitable for this purpose may be defined by the balance of few reactions (Eqs 1, 2, 3, 4, and 5) that occur when CO_2 dissolves in sea water [13–15] as shown below:

$$CO_{2(g)} = CO_{2(aq)}, \tag{1}$$

$$CO_{2(aq)} + H_2O_{(l)} = H_2CO_{3(aq)}, \tag{2}$$

$$H_2CO_{3(aq)} = H^+_{(aq)} + HCO^-_{3(aq)}, \tag{3}$$

$$HCO^-_{3(aq)} = H^+_{(aq)} + CO^{2-}_{3(aq)}, \tag{4}$$

$$CO^{2-}_{3(aq)} + Ca^{2+}_{(aq)} = CaCO_{3(s)}, \tag{5}$$

Ocean acidification data (pH, TA, $[HCO_3^-]$ $[H_2CO_{3(aq)}]$ $[CO_{2(aq)}]$ ρCO_2, Ω_{Calc}, and Ω_{Arag}) are also indispensable for validating CO_2 modeling tests on both a global and regional scale.

Studies on water masses in northeastern Brazil are scarce, but some previous studies in the South Atlantic indeed covered the surface (0–200 m), intermediate (200–1000 m), and deep (below 1000 m depth) waters. Reid [16], estimated the general circulation pattern of the South Atlantic from the characteristics of the geostrophic shear, reporting contributions from North Atlantic waters. Some authors [16–21] investigated the physical-chemical characteristics (temperature, salinity, and oxygen) of the different water masses in the South Atlantic, disregarding the chemistry of the carbonate system. Apart from these works are those by Silveira [20], Campos et al. [22], and Silva [19] in the southeastern region of Brazil, but these works did not deal with the carbonate system. By contrast, Bates [23], studied the distribution of carbonate chemistry in samples collected from many water masses in the Southeast Pacific as part of the US GEOTRACES project, compared with the carbonate chemistry from samples collected 20 years earlier in the same area. Also, several recent studies with the carbonate system have been carried out in coastal waters on the Brazilian continental shelf in northeast-south-southeast regions [1, 13, 14, 22–26].

The present study aimed to compile, in an unprecedented way, an inventory of the carbonate system in water masses of the northeast margin of Brazil (Tropical Water, South Atlantic Central Water, Antarctic Intermediate Water, and Upper North Atlantic Deep Water) and to elucidate the physical-chemicals processes governing these concentrations and speciation. In addition, to verify the dynamics of the carbonate system parameters through the program Marine Chemical Analysis (AQM). This experiment provides information and encourages ocean acidification monitoring projects.

Materials and method

Study area

The study area is located on the northeastern continental margin of Brazil, in the sedimentary Sergipe/Alagoas (SEAL) basin. The SEAL basin is divided between terrestrial and maritime domains, comprising an oil province in an advanced exploratory stage that gives economic and environmental importance to the vicinity [25]. The terrestrial domain of the basin comprises the states of Sergipe and Alagoas, which are separated by the course of the São Francisco River (Fig 1). The maritime part of the SEAL occurs along the continental shelf, which is 20 to 50 km long, and the platform slope, which occurs between 40 and 80 m deep [25]. In this context, the present study covered an extension of 350 km from the coastline, where the Tropical Water and Coastal Water are the predominant water masses [26].
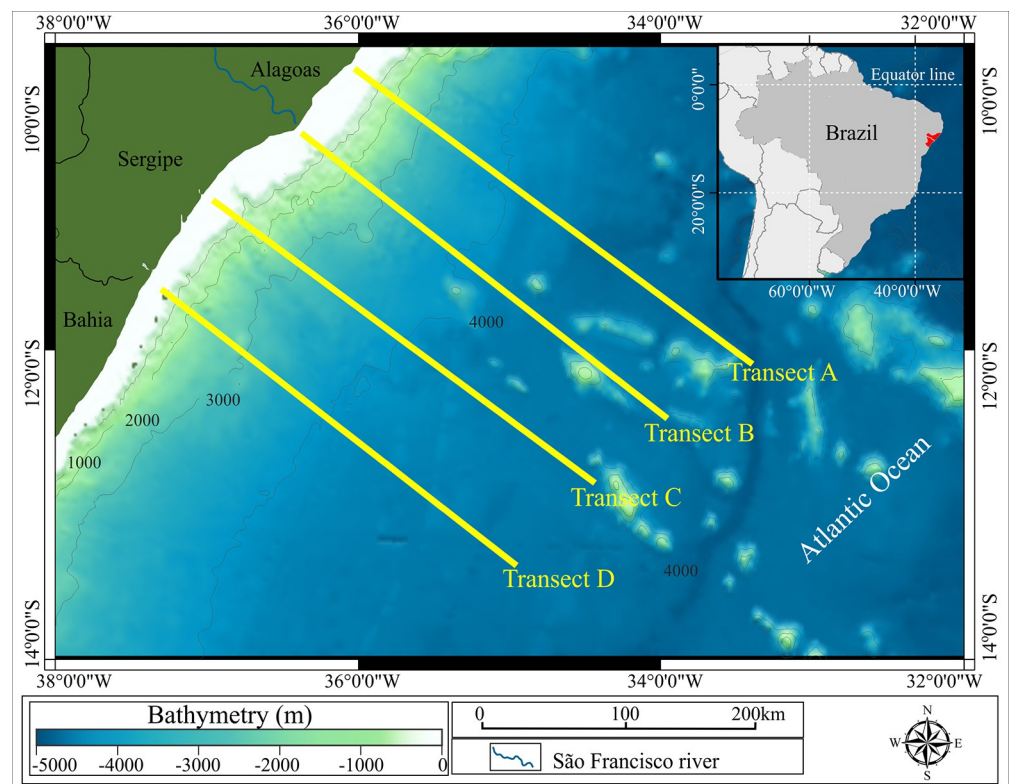

Fig 1. Reference map of the study site. Northeastern continental margin of Brazil, within the Sergipe–Alagoas sedimentary basin. Blue shades, local depth; yellow lines, sampling transects A, B, C, and D; blue line, São Francisco river; dark green filled shape, Brazilian states that are adjacent to transects.

https://doi.org/10.1371/journal.pone.0271875.g001

Data acquisition

The samples were collected between May 10 and 21, 2014, which is the beginning of the rainy season (127 mm^3/month) [27]. The sampling effort took place onboard the R/V Seward Johnson during a cruise through the SEAL basin, which was made possible by financial resources and logistical support provided by the MARSEAL Project (PETROBRAS/CENPES). Collection of the samples was conducted through a CTD (conductivity, temperature, and depth sampler) coupled to a *Rosette* with capacity for 24 oceanic bottles of the Niskin and Go-Flo type (General Oceanics brand).

The collections were conducted along four transects (A, B, C, and D, Fig 1), arranged latitudinally. In each transect, eight to nine stations were established, totaling 34 profiles, with a maximum distance of 365 km from the shoreline (Table 1).

Sampling depths were established from six isobaths, *i.e.*, 5, 20, 250, 700, 1250, and 1650 m, that correspond to the current water mass's system in the South Atlantic (TW, Tropical Water; SACW, South Atlantic Central Water; AAIW, Antarctic Intermediate Water; and UNADW, Upper North Atlantic Deep Water), according to Silveira [20]. The boundaries within each water layer were determined from the CTD data (Table 2), which were also used to conduct the T-S (temperature–salinity) diagram.

For each collection station, different sampling depths were defined according to the CTD information (T-S diagram), allowing for the identification of the interfaces between the different water masses (Fig 2); further information can be found on the S1 Table.

Table 1. Profiling stations by transect A, B, C, and D. Station: Identification number; Dist: Distance from the shoreline to each station (km).

A		B		C		D	
Station	**Dist**	**Station**	**Dist**	**Station**	**Dist**	**Station**	**Dist**
1	8	38	4	39	6	75	12
2	21	37	8	40	14	74	19
3	25	36	12	41	25	73	23
4	30	35	19	42	29	72	30
8	83	33	34	43	36	68	68
10	127	29	86	47	81	66	97
14	247	27	116	49	111	62	216
18	365	23	219	53	230	58	335
		19	340	57	349		

https://doi.org/10.1371/journal.pone.0271875.t001

Table 2. Fieldwork recognition of the water masses (Wm). Thermohaline limits, sampling depths, and referential depths [20].

Wm	Temperature (˚C)	Salinity (g/kg)	Sampling depth (m)	Wm depths (m) [31]
MW[1]	27.91	35.56	4.3	–
TW[2]	27.37–28.26	36.44–37.55	4–21	0–142
SACW[3]	13.33–15.59	35.41–35.78	202–299	142–567
AAIW[4]	4.12–5.59	34.53–34.93	598–1250	567–1060
AAIW/UNADW	3.89–4.37	34.70–35.13	999–1650	1060–1300
UNADW[5]	3.56–4.28	35.09–35.13	1398–1899	1300–3260

[1]Mixture Water.

[2]Tropical Water.

[3]South Atlantic Central Water.

[4]Antarctic Intermediate Water.

[5]Upper North Atlantic Deep Water.

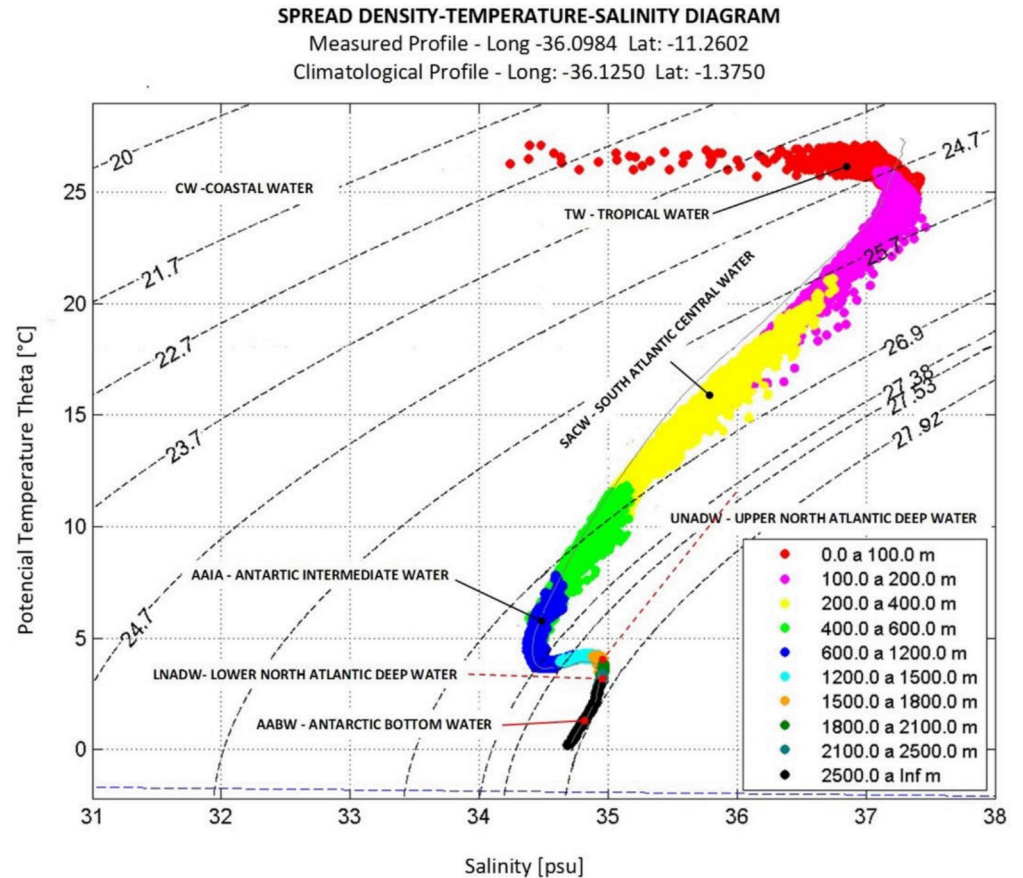https://doi.org/10.1371/journal.pone.0271875.t002

Fig 2. T-S diagram indicating the distinct water masses from the studied area (maritime sedimentary SEAL basin).

Thermodynamic modeling

The modeling and the procedural calibrations described in this manuscript were performed with the Marine Chemical Analysis (AQM) program [1]. The AQM is a package of thermodynamic equations, executed via MS Excel, which can predict the complex composition of the marine carbonate system based on measurements that can be made relatively inexpensively such as pH, temperature, and alkalinity reducing the overall costs of ocean acidification monitoring programs. The AQM program is available upon request to the corresponding author's email.

Statistical procedure

Data normality was verified using the Shapiro-Wilks test, and based on this result, the non-parametric Kruskal Wallis test was chosen for comparisons between groups. All statistical tests were performed using the Statistica 7.0 software (TIBCO) with a significance level set at $p < 0.05$.

Analytical procedure

The analytical method was based on international procedures for studies involving the chemistry of inorganic carbon dioxide in marine waters [11, 28–32] with the necessary adaptations (S2 Table).

T-S diagram

Temperature and salinity data from CTD profiling were utilized to make the profiles and vertical sections of temperature, salinity, and potential density of the stations using the T-S diagram. The water masses were aimed to be determined by mapping their interfaces, characterizing their core, and isopycnals. The optimal multiparametric analysis was utilized to provide data on the interface limits and at the average core depth of each water mass. This allowed locating each layer in the T-S diagram parameterized by the depth range associated with its typical values of temperature, salinity, and potential density [33, 34]. The density of the water masses was displayed as isopycnals on the T-S diagram.

Absolute salinity (S_A). The S_A (g/kg) was calculated from the electrical conductivity measured *in situ* (CTD) and the thermodynamic equation of seawater [35]. Absolute salinity is the most accurate parameter established to estimate the real salinity of the environment. Unlike other scales (for example, conductivity and practical salinity), S_A also considers the non-electrolytic salts through algorithms extracted from the data on the water's chemical composition in a given region [35].

TA. For the determination of TA, water samples were collected and filtered in a Nalgene filtration system through GF/F filters before being transferred to BOD type flasks (300 mL, from the Kimble brand) and immediately analyzed [28].

The potentiometric determination was conducted with duplicate samples in an open thermostated glass cell, where 3 mL (to obtain v1) and 10 mL (to obtain v2) of HCl 0.1 M were added to each 100 mL sample [36]. The method consists in determining the slope of the line by obtaining two points for the function of Gran (F): F (1) defined by v1 and F (2) defined by v2 [36]. A Thermo Scientific Orion Star potentiometer coupled to the Orion glass reference electrode cell, model 8102BNUWP was used for potentiometric determinations. The pH electrode was calibrated daily with "Tris" buffer (0.04 m) for sample readings (maximum 15 samples per day). Due to the reduced number of samples per day, the short period of the oceanographic cruise, and the constant working conditions (electricity source, solutions, and equipment), we chose to verify the electrode performance at the beginning and the end of the oceanographic cruise. The electrode's percent efficiency ranged between 99.49% and 99.54% concerning the theoretical Nernst value (59 mV). More details are available in hydrogen potential (pH).

The analytical precision and accuracy were calculated from five replicates of the reference material (Dickson–CRM, for oceanic CO_2 measurements, batch 104) [37], which obtained a 95% recovery rate from the expected value (Table 3). The calculated TA was obtained by the AQM program through the equation (TA (µmol/kg) = 660 + 47.6S) defined by Hunter [38] for waters of the Atlantic and Pacific oceans by the GEOSECS Program. The normalized total alkalinity (NTA) was obtained by the AQM program using the equation (NTA (µmol/kg) = TA (µmol/kg)x35/Salinity (g/kg), 35 was assumed to be the representative salinity of the water masses.

Hydrogen potential (pH). The total pH of the water samples collected during the cruise was determined in the R/V Seward Johnson "wet laboratory" as follows: pH_T (= -log([H^+] + [(HSO_4^-)/c^o), where c^o is the thermodynamic concentration (1 mol/kg-soln).

Table 3. Total alkalinity measured from 5 replicates of the certified reference material (Dickson, oceanic CO_2 measurements, batch 134).

	Expected value	Measured value	Accuracy		Precision	Sample volume
		Average (n = 5)	Absolute error	Relative error	Variation coefficient	mL
Total alkalinity	2222.6 µmol/kg	2108.0 µmol/kg	−115.0	−5.0	1.66%	50

The internal solution of the combined pH electrode was filled up with 0.7 m NaCl to reduce the potential liquid junction. The electromotive force (emf) of the electrode was related to the molar concentration of the proton [H$^+$], as shown in Eq 6.

$$E = E^\circ - \left(\frac{RT}{F}\right)\ln[H^+], \tag{6}$$

where E˚ is the standard electrode potential, which was determined by titrating a 0.7 m NaCl solution with 0.179 M HCl [29]. The pH$_T$ (total scale) values were measured immediately after each collection at a constant temperature of 25˚C in a thermostatic cell connected to a micro-processed thermostatic bath with external circulation (Qimis) to avoid temperature bias [39]. The determinations were made by the Thermo Scientific Orion Star potentiometer coupled to the Orion glass reference electrode with a 0.7 m NaCl outer chamber filling solution, model 8102BNUWP. The analytical slope for the electrode was within ± 0.13 mV (teoretical Nersnt value at 25˚C). The electrode was calibrated with a "Tris" buffer (0.04 m) prepared in the laboratory [40], where pH values were assigned by spectrophotometry (m-cresol method) [14, 28, 41]. The "Tris" buffer allows accuracy of 0.001 pH units [40, 42]. Subsequently, using the AQM program, the pH results were corrected for the temperature recorded at the sampling moment (pH$_t$ = pH$_{25}$ + A + Bt + Ct^2) [43].

Calcium (Ca) and total boron (B$_T$). The determination of Ca and B$_T$ was conducted using a MIP OES (microwave-induced plasma optical emission spectrometer, 4200 MP-AES, Agilent brand). The external analytical curves were made with monoelementary standards (1000 mg/L, VHG®) with concentrations in the range of 0.1 to 10 mg/L, in an ultrapure water matrix. A matrix influence test was conducted in which it was found that both the boron and calcium signals did not show any significant difference between the ultrapure water matrices and the 500 mg/L NaCl solution. The calculated calcium and boric acid were also obtained using the equations described by Millero, respectively [44, 45]; [Ca^{2+}]$_T$ = 2.938x10^{-4}xS, [B]$_T$ = 0.000416x(S/35).

CO$_2$ inorganic system. All parameters from the inorganic CO$_2$ system (CO$_2$, CO$_3^{2-}$, HCO$_3^-$, DIC, ρCO$_2$, Ω$_{Calc}$, and Ω$_{Arag}$) were calculated using the carbonate system dissociation constant K [46] defined as follows:

- lnk_B^* [37]

- lnk_{Si}^* [45]

- lnk_1^* (H$_3$PO$_4$) [47]

- lnk_2^* (H$_2$PO$_4^-$) [47]

- lnk_3^* (HPO$_4^{2-}$) [47], and

- lnk_2^* (CO$_3^{2-}$) [48].

The aqueous concentrations (CO$_{2(aq)}$) and the partial pressure (ρCO$_2$) were calculated from the variables of temperature, salinity, pH, and TA and by using the thermodynamic and stoichiometric constant K (pk$_1^\circ$, pk$_2^\circ$, pk$_1^*$, and pk$_2^*$) [10, 49]. The AQM was also used in this phase, aiding the calculations.

Results and discussion

T-S diagram

The identification of water masses was conducted via the T-S diagram (Fig 2) methodology, which uses the temperature and salinity data [50] to obtain the depth boundaries of water masses.

Table 4. Temperature (˚C) and salinity (g/kg) for each water mass (Wm). Comparison with previously published results.

Wm	Temperature (˚C)	Salinity (g/kg)	Reference
TW	27.37–28.36	36.44–37.55	**The present study**
	>20.00	>36.17	[51]
	>20.00	>36.37	[20]
	>18.00	>36.17	[19]
	20.00–27.00	–	[52]
SACW	13.33–15.59	35.42–35.78	**The present study**
	5. 00–20.00	34.46–36.17	[52]
	8.72–20.00	34.82–36.37	[20]
	6.00–20.00	34.76–36.17	[53]
	10.00–20.00	35.16–36.17	[51]
	–	34.81–36.17	[54]
	5.95–18.35	34.68–36.57	[19]
AAIW	4.12–5.59	34.53–34.93	**The present study**
	3.46–8.72	34.58–34.82	[20]
	4.92–5.90	34.64–34.94	[19]
NADW	3.56–4.37	35.09–35.13	**The present study**
	3.00–4.00	34.76–35.16	[53]
	2.04–3.31	34.75–35.03	[20]

In this way, an existing variation in our temperature and salinity values could be perceived with those of the other authors mentioned in Table 4. Furthermore, the Upper Circumpolar Deep Water was not addressed in this work because of the complexity of its definition, such as the oxygen and nutrients concentrations, to differentiate this water mass with the overlying (AAIW) and underlying (UNADW) masses [20].

The salinity from the superficial layer (4.3 m deep) of station 36 was lower than the expected value (>36.37 g/kg) for a TW mass [20]. A continental freshwater input may explain this difference; thus, this sample was called "Mixture Water" (MW).

Measured versus predicted values

Calcium and total boron. The values analyzed and calculated in the different water masses varied below 5% for calcium (Ca^{2+}) and between 7.03% and 18.94% for total boron (B_T) (Table 5).

In this validation step, the calculated (AQM) concentrations for calcium and boron emphasized that these values may be recommended instead of those obtained analytically to investigate

Table 5. Calcium and total boron concentrations (µmol/kg; mean ± standard deviation) in water samples from 34 stations. Analytically obtained levels: microwave-induced plasma atomic emission spectrometry. Predicted concentrations: calculated using the AQM program using the absolute salinity scale (g/kg). When calculating the relative error (RE%), the expected value is the analyzed value.

Wm	Sample Sizes	Ca^{2+} analyzed	Ca^{2+} calculated	RE (%)	B_T analyzed	B_T calculated	RE (%)
MW	*n = 1	10180	10664	**4.75**	357	410	**14.91**
TW	*n = 63	11168 ± 199	11210 ± 63	**0.38**	383 ± 23	410 ± 0.04	**7.03**
SACW	*n = 24	10570 ± 221	10716 ± 33	**1.39**	362 ± 26	412 ± 0.08	**13.77**
AAIW	*n = 22	10203 ± 163	10417 ± 26	**2.10**	347 ± 26	412 ± 0.02	**18.94**
AAIW/UNADW	*n = 18	10287 ± 154	10540 ± 28	**2.46**	353 ± 36	412 ± 0.02	**16.86**
UNADW	*n = 15	10303 ± 227	10587 ± 3	**2.76**	352 ± 36	412 ± 0.01	**16.99**

RE = relative error.

Table 6. Variations in the carbonate system parameters as a function of the minimum (a, c) and maximum (b, d) values found for Ca^{2+} and B_T (Table 5). Values obtained with the AQM program keeping the temperature (25˚C), salinity (35 g/kg), pH_T (8.0), and TA (2300 µmol/kg) variables constant at the program entry. The expected value is the analyzed value.

	CA µmol/kg	Ω_{Calc}	Ω_{Arag}	HCO_3^- µmol/kg	CO_3^{2-} µmol/kg	DIC µmol/kg	CO_2 µmol/kg
Ca^{2+} (a)	2173	5.0	3.3	1704	210	1921	12.0
Ca^{2+} (b)	2173	5.2	3.5	1704	210	1921	12.0
Δ% (b-a)	0.0	4.0	6.1	0.0	0.00	0.0	0.0
B_T (c)	2173	5.0	3.3	1704	210	1931	12.0
B_T (d)	2160	5.0	3.3	1694	209	1914	12.0
Δ% (d-c)	-0.6	0.0	0.0	-0.6	-0.5	−0.86	0.0

(a) 10180 µmol/L (analyzed), (b) 10664 µmol/L (calculated), represent the largest RE (%) in the Table 5. (c) 347 µmol/L (analyzed); (d) 412 µmol/L (calculated).

CA = carbonate alkalinity (TA-ΣBi; Bi = bases). The analyzed and calculated values were obtained from Table 5, with the highest RE (%).

https://doi.org/10.1371/journal.pone.0271875.t006

the carbonate system involving the same water masses. Calcium concentration is important for the equations that determine the saturation state of calcite. The concentration of boron allows obtaining, through equations, the concentrations of carbonate alkalinity $[CO_2]$, $[CO_3^{2-}]$, $[HCO_3^-]$, and DIC [10, 28]. The variation presented for Ca (analyzed and calculated) did not show relevant interference in the predicted values for the carbonate system (Table 6). Regarding the total estimated boron, despite having a variation of 18.94%, relative to the analyzed value, we also recommend its application for studies of the carbonate system in these water masses, since the concentrations obtained through the calculated B_T showed tiny variation (<1%) (Table 6).

Practical versus absolute salinity. The S_A (g/kg) has been considered the most accurate measure to estimate the real salinity of the environment [35]. However, practical salinity unit (psu) has been widely used by researchers to generate carbonate system values [1, 6, 14, 15, 55]. Thus, the AQM program was fed with both the psu and g/kg salinity scales to test the existence of relevant interference when predicting the carbonate system fractions (obtained from the analytical TA) from the studied water masses (Table 7).

It was not evident in this process that the S_A is the most suitable scale for calculations of the carbonate system, mainly for speciation and concentration of the carbonate, where the effect of salinity did not generate an error of more than 1% between the different water masses studied, except for the MW, that presented variations above 4% for NTA (n = 1). Regarding Ca^{2+} e B_T's calculation from the practical and absolute salinity, the RE was between 0.5% and 0% for Ca^{2+} and B_T, respectively. Although S_A represents the better estimation of the salinity, it does not influence the equations that generate Ca^{2+}, B_T, and TA (Table 7). The use of practical or absolute salinity in the total boron calculation equation resulted in irrelevant differences in this study. However, more verification and experimental confirmation are needed for these water masses, mainly in the MW, where the number of samples was quite small (n = 1). The total average of the B_T/Cl ratio ((mg/kg)/Cl/‰) for all water masses was 0.223 (for calculated B_T) and 0.199 (for analyzed B_T), being similar to that found (0.232) by Uppström [56]. More water collections in the studied are necessary to establish a better empirical relationship between B_T and S. Kulinski et al. [57] established this empirical relationship for the calculations of the carbonate system in the Baltic Sea.

The relative error in Table 8 varies between 5.0 and 6.5% for the analyzed and calculated TA values. The relationship between TA and salinity is well known, and several researchers have proposed empirical equations [38, 58, 59]. In this study, the differences between the predicted values and the measured values are somewhat high compared to those presented by Jiang et al. [60], but this may be due to applied equation and small sample size (n<65). New samples were already collected during the dry season and are currently being analyzed. This

Table 7. Effects of the practical (psu) and absolute salinity (g/kg) scales when generating the carbonate system parameters. Values obtained from calculated total alkalinity with the AQM program [1, 13–15]. Further information can be found in the methodology section. In calculating the relative error (RE%), the parameters obtained by the absolute salinity (g/kg) are the expected values.

Parameters	Water mass					
	MW	TW	SACW	AAIW	AAIW/UNADW	UNADW
Ca^{2+} (psu)	10613	11156 ± 63	10665 ± 33	10365 ± 26	10488 ± 28	10536 ± 3
Ca^{2+} (g/kg)	10664	11210 ± 63	10716 ± 33	10417 ± 26	10540 ± 28	10587 ± 3
RE (%)	**-0.5**	**-0.5**	**-0.5**	**-0.5**	**-0.5**	**-0.5**
B_T (psu)	410	410 ± 0.0	412 ± 0.1	412 ± 0.0	412 ± 0.0	412 ± 0.0
B_T (g/kg)	410	410 ± 0.0	412 ± 0.1	412 ± 0.0	412 ± 0.0	412 ± 0.0
RE (%)	**0.00**	**0.00**	**0.00**	**0.00**	**0.00**	**0.00**
TA (psu)	2345	2429 ± 9.7	2347 ± 5.4	2298 ± 3.9	2317 ± 4.4	2324 ± 0.4
TA (g/kg)	2352	2437 ± 9.7	2355 ± 5.4	2306 ± 4.0	2325 ± 4.4	2332 ± 0.4
RE (%)	**-0.3**	**-0.3**	**-0.3**	**-0.3**	**-0.3**	**-0.3**
NTA (psu)	2242	2194 ± 42	2235 ± 11	2280 ± 9	2263 ± 11	2262 ± 19
NTA (g/kg)	2232	2184 ± 42	2224 ± 11	2269 ± 9	2252 ± 11	2251 ± 19
RE (%)	**4.3**	**0.5**	**0.5**	**0.5**	**0.5**	**0.5**
Ω_{Calc} (psu)	5.47	5.78 ± 0.27	3.30 ± 0.26	1.95 ± 0.28	1.72 ± 0.16	1.72 ± 0.13
Ω_{Calc} (g/kg)	5.42	5.81 ± 0.26	3.27 ± 0.26	1.93 ± 0.28	1.71 ± 0.16	1.70 ± 0.12
RE (%)	**0.9**	**-0.5**	**0.9**	**1.0**	**0.6**	**1.2**
Ω_{Arag} (psu)	3.64	3.85 ± 0.18	2.12 ± 0.17	1.23 ± 0.18	1.08 ± 0.10	1.08 ± 0.08
Ω_{Arag} (g/kg)	3.61	3.82 ± 0.18	2.10 ± 0.17	1.22 ± 0.18	1.08 ± 0.10	1.08 ± 0.08
RE (%)	**0.8**	**0.8**	**1.0**	**0.8**	**0.0**	**0.0**
CO_3^{2-} (psu)	231.18	238 ± 11	137 ± 10	81 ± 12	71 ± 6	72 ± 5
CO_3^{2-} (g/kg)	231.69	238 ± 11	136 ± 10	81 ± 12	71 ± 6	72 ± 5
RE (%)	**−0.2**	**0.0**	**0.7**	**0.0**	**0.0**	**0.0**
DIC (psu)	1873	1822 ± 43	2019 ± 21	2115 ± 20	2112 ± 18	2109 ± 19
DIC (g/kg)	1883	1813 ± 43	2009 ± 21	2105 ± 20	2102 ± 18	2099 ± 19
RE (%)	**−0.5**	**0.5**	**0.5**	**0.5**	**0.5**	**0.5**
CO_2 (psu)	10.77	10 ± 1	18 ± 2	31 ± 5	34 ± 3	34 ± 3
CO_2 (g/kg)	10.82	10 ± 1	18 ± 2	31 ± 5	34 ± 3	34 ± 3
RE (%)	**-0.5**	**0.0**	**0.0**	**0.0**	**0.0**	**0.0**
	*n = 1	*n = 63	*n = 24	*n = 22	*n = 18	*n = 15

Concentrations are in µmol/kg; psu = practical salinity unit; g/kg = absolute salinity.

*n = sample size.

Table 8. Variations in TA (µmol/kg) were obtained analytically and calculated with the AQM program [1, 13–15]. In calculating the relative error (RE%), the values obtained analytically are the expected values (see item Analytical Procedure: TA and Table 3).

Parameters	Water mass					
	MW	TW	SACW	AAIW	AAIW/UNADW	UNADW
TA (a)	2232	2289 ± 44	2219 ± 14	2197 ± 10	2205 ± 10	2213 ± 19
TA (b)	2352	2437 ± 10	2355 ± 5	2306 ± 4	2325 ± 4	2332 ± 0.4
RE (%)	**5.3**	**6.5**	**6.1**	**5.0**	**5.4**	**5.4**
	*n = 1	*n = 63	*n = 24	*n = 22	*n = 18	*n = 15

(a) = analyzed; (b) = calculated

*n = sample size.

will allow the development of specific empirical equations for these water masses with smaller differences between predicted and measured values.

Inventory and elucidation of physical–chemical processes

Carbonate system composition and speciation (pH, NTA, and DIC). The pH and NTA values showed significant variations between the different water masses (coefficient of variation = 1.13% and 1.92%, respectively). In Figs 3 and 4, a drop in pH values can be observed according to the following sequence: TW > SACW > AAIW > AAIW/UNADW < UNADW. The lowest pH value was found in the AAIW/UNADW (7.83) and the highest ones in the TW (8.02). The increase in the content of HCO_3^- and CO_2 at greater depths may be due to the decomposition of organic matter by respiratory activity [59]. The drop in pH values can be explained by the release of protons from the reaction (Eq 7) between CO_2 and seawater, forming bicarbonate [15] (Fig 3).

$$CO_2 + H_2O = HCO_3^- + H^+ \tag{7}$$

In the present study, the water masses had a buffering capacity (ability to keep the pH stable while acids are added) well above the minimum capacity, if considering that TA/DIC = 1. The minimum buffering capacity occurs when the pH value falls close to 7.5 [59], and consequently, the carbonate concentrations are lower.
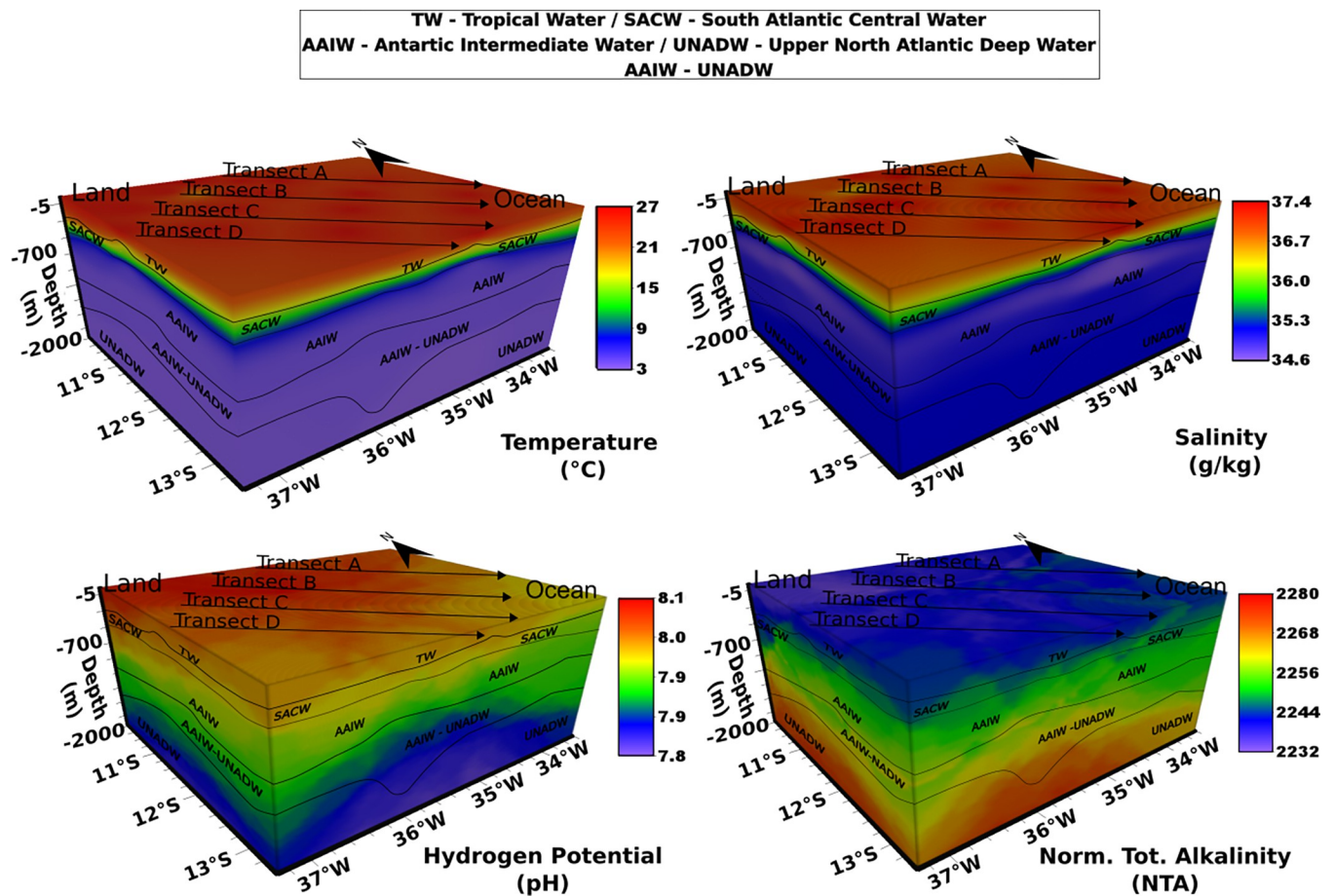

Fig 3. Temperature, Salinity, pH, and Normalized Total Alkalinity (NTA) of the sampling transects, from the internal platform to the abyssal plain.
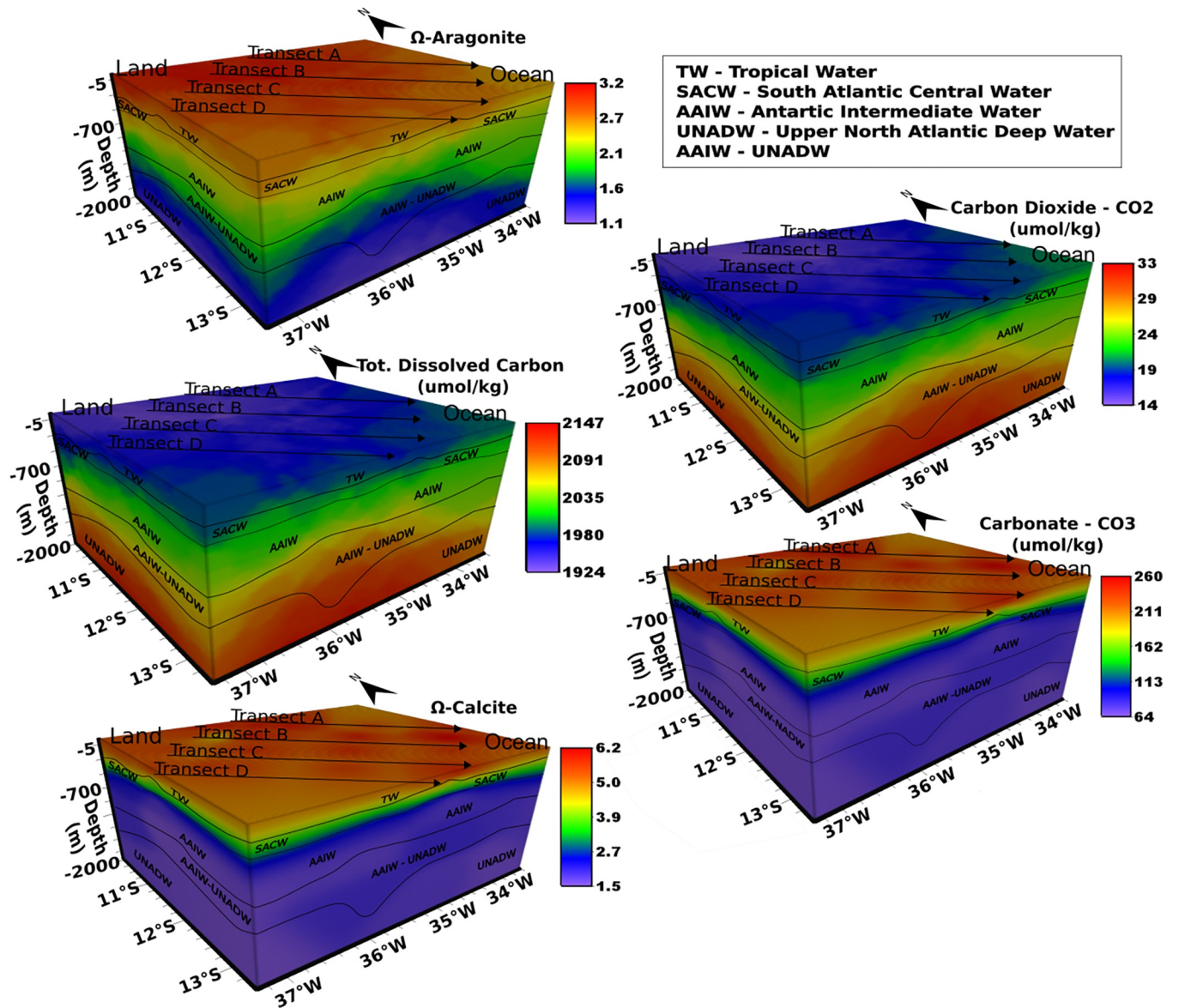
Fig 4. Aragonite saturation state (S-Aragonite), carbon dioxide, total dissolved carbon (DIC), carbonate, and calcite saturation state (S-Calcite) from sampling transects: From the internal platform to the abyssal plain.

https://doi.org/10.1371/journal.pone.0271875.g004

All pH values presented here were well above 7.8, whereas the NTA concentration of the five water masses showed values of approximately 2200 μmol/kg. Conversely, DIC amounts in distinct water masses showed a 7% coefficient variation, ranging between the minimum of 1845 μmol/kg (TW) and a maximum of 2020 μmol/kg (SACW). Moreover, our data showed raised DIC values for deeper water masses with increasing concentrations of HCO_3^- and CO_2 (r = 0.95; r = 1.00, respectively; p<0.05), Fig 4.

Average concentrations of HCO_3^- and CO_2 showed an increase relative to greater depths in the following sequence (values are in μmol/kg):

$$TW \ (HCO_3^- = 1594; \ CO_2 = 10) < SACW \ (HCO_3^- = 1864; \ CO_2 = 18) < AAIW \ (HCO_3^- = 2037; \ CO_2 = 31)$$
$$< AAIW/UNADW \ (HCO_3^- = 2040; \ CO_2 = 34) < UNADW \ (HCO_3^- = 2038; \ CO_2 = 34)$$

.

The increase in the content of HCO_3^- and CO_2 at greater depths may be due to the decomposition of organic matter by respiratory activity [61].

Calcite and aragonite saturation state. The saturation state of calcite (Ω_{Calc}) and aragonite (Ω_{Arag}) varied within water masses. The highest values were observed in TW and SACW for both minerals, respectively: Ω_{Calc} = 5.8, Ω_{Arag} = 3.9 and Ω_{Calc} = 3.3, Ω_{Arag} = 2.1. From the AAIW, the values dropped by almost half (Ω_{Calc} = 2.0 and Ω_{Arag} = 1.2). The increase in CO_2 concentrations is mainly responsible for this scenario since it may raise the carbonic acid content. The following reaction (Eq 3) characterizes the main buffering capacity of seawater, where the consumption of H^+ and CO_2 occurs. As the carbonate is consumed from seawater by this reaction (Eq 8), it results in a decreased carbonate saturation state [59].

$$CO_2 + CO_3^{2-} + H_2O = 2HCO_3^- \tag{8}$$
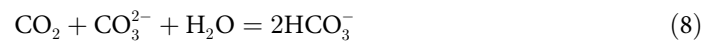
Several authors have linked the calcium saturation state (Ω) with the calcification capacity of organisms due to a drop in CO_3^{2-} availability [62–64], Eq 9. Moreover, previous experiments reported a positive correlation between the calcification rate and Ω, which may lead to an erroneous idea that CO_3^{2-} governs the calcification rate [65, 66].

$$\Omega = \frac{[Ca^{2+}][CO_3^{2-}]}{Kps} \tag{9}$$

Recent research [4, 67, 68] suggested that Ω from seawater does not control the rate of calcification (calcifying fluid). That is, we cannot merely link the availability of carbonate (affected by the decrease in pH values) to the rate of calcification. Notably, to date, no CO_3^{2-} transporter has been found in calcifying organisms (for example, coccolithophorids). Conversely, there is ample evidence of HCO_3^- transporters. The bicarbonate within the calcifying fluid provides for the formation of calcium carbonate, Eq 10.

$$HCO_3^- + Ca^{2+} = H^+ + CaCO_3 \tag{10}$$
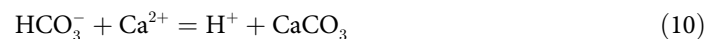
Reactions involving the formation of calcium carbonate are dependent on the electrochemical gradient (H^+) between the marine environment and the organisms' tissue, as well as suitable Ω (higher) in the cytoplasmic fluid. Several gaps still need to be clarified about calcification of marine organisms [69–71].

From the above, pH is a valuable measure by its participation in various chemical equilibrium reactions (proton concentration) [31, 32]. Thus, accurate data on the speciation and quantification of the carbonate system can be obtained at reduced costs [31, 72].

Conclusions and future perspectives

The present inventory of the carbonate system in the five water masses in the SEAL marine sedimentary basin showed a well-defined scenario among these masses regarding pH, Ω, CO_3^{2-}, DIC, and CO_2. The variation of these parameters over time remains unknown, requiring seasonal sampling efforts to allow comparisons between water masses. Through a robust and updated database, these parameters can be used to monitor the marine acidification of the studied area at a reduced cost and effort.

More experiments are needed in the studied area to establish more precise empirical relationships between the different parameters of the carbonate system, such as B_T vs. S, Ca vs. S and TA vs. S. These relationships may be suitable for future studies of the carbonate system of these and other water masses. This tool may one day replace the laboratory determinations of

TA, calcium, and boron since the carbonate system presents slight variation between the calculated and analyzed values, making the whole process more agile and reducing costs.

Supporting information

S1 Table. Sampling stations for the oceanographic cruise in the Sergipe-Alagoas sedimentary basin held in May 2014 on board the Seward Johnson research vessel.
(PDF)

S2 Table. Dataset for the manuscript "Inventory of water masses and carbonate system from Brazilian's northeast coast: Monitoring ocean acidification". ID Number = is the identification number of the sample, it is related to the sampling samples. Group = is the number of samples (n) per water mass. psu = is the practical salinity unit; S‰ = is the absolute salinity; (A) = analyzed values and (C) = calculated values. Latitude and Longitude are the geographical positions (Geographic Coordinates in decimal degrees, Datum SIRGAS 2000).
(XLSX)

Acknowledgments

Author Contributions

Conceptualization: Carlos Augusto Ramos e Silva.

Data curation: Carlos Augusto Ramos e Silva, Nicole Silva Caliman Monteiro, Luciana Miranda Cavalcante.

Formal analysis: Carlos Augusto Ramos e Silva, Flavo Elano Soares de Souza, Carlos Alexandre Borges Garcia.

Funding acquisition: Carlos Augusto Ramos e Silva, Carlos Alexandre Borges Garcia.

Investigation: Carlos Augusto Ramos e Silva, Nicole Silva Caliman Monteiro, Luciana Miranda Cavalcante, Waldemar Tavares Junior, Maria Eulália Rocha Carneiro, Flavo Elano Soares de Souza, Carlos Alexandre Borges Garcia, Raimundo Nonato Damasceno, Anderson de Araújo Rocha.

Methodology: Carlos Augusto Ramos e Silva, Nicole Silva Caliman Monteiro, Luciana Miranda Cavalcante, Waldemar Tavares Junior, Flavo Elano Soares de Souza, Carlos Alexandre Borges Garcia, Raimundo Nonato Damasceno, Anderson de Araújo Rocha.

Project administration: Carlos Augusto Ramos e Silva, Carlos Alexandre Borges Garcia.

Software: Carlos Augusto Ramos e Silva.

Supervision: Carlos Augusto Ramos e Silva.

Validation: Carlos Augusto Ramos e Silva, Luciana Miranda Cavalcante, Waldemar Tavares Junior, Maria Eulália Rocha Carneiro, Flavo Elano Soares de Souza, Anderson de Araújo Rocha.

Visualization: Carlos Augusto Ramos e Silva, Luciana Miranda Cavalcante, Waldemar Tavares Junior, Maria Eulália Rocha Carneiro, Flavo Elano Soares de Souza, Raimundo Nonato Damasceno, Anderson de Araújo Rocha.

Writing – original draft: Carlos Augusto Ramos e Silva, Nicole Silva Caliman Monteiro, Luciana Miranda Cavalcante, Maria Eulália Rocha Carneiro.

Writing – review & editing: Carlos Augusto Ramos e Silva.

References

1. Ramos e Silva CA, Dávalos PB, Da Silva MP, Miranda LB de. Variability and Transport of Inorganic Carbon Dioxide in a Tropical Estuary. J Oceanogr Mar Res. 2017; 05: 155. https://doi.org/10.4172/2572-3103.1000155

2. Ver LMB, Mackenzie FT, Lerman A. Biogeochemical responses of the carbon cycle to natural and human perturbations: Past, present, and future. Am J Sci. 1999; 299: 762–801. https://doi.org/10.2475/ajs.299.7–9.762

3. Cai WJ, Hu X, Huang WJ, Murrell MC, Lehrter JC, Lohrenz SE, et al. Acidification of subsurface coastal waters enhanced by eutrophication. Nat Geosci. 2011; 4: 766–770. https://doi.org/10.1038/ngeo1297

4. Cyronak T, Schulz KG, Jokiel PL. The Omega myth: What really drives lower calcification rates in an acidifying ocean. ICES J Mar Sci. 2016; 73: 558–562. https://doi.org/10.1093/icesjms/fsv075

5. Pendleton L, Comte A, Langdon C, Ekstrom JA, Cooley SR, Suatoni L, et al. Coral reefs and people in a high-CO2 world: Where can science make a difference to people? PLoS One. 2016; 11: 1–21. https://doi.org/10.1371/journal.pone.0164699 PMID: 27828972

6. Réveillac E, Lacoue-Labarthe T, Oberhänsli F, Teyssié JL, Jeffree R, Gattuso JP, et al. Ocean acidification reshapes the otolith-body allometry of growth in juvenile sea bream. J Exp Mar Bio Ecol. 2015; 463: 87–94. https://doi.org/10.1016/j.jembe.2014.11.007

7. Fabry VJ, McClintock JB, Mathis JT, Grebmeier JM. Ocean acidification at high latitudes: The Bellwether. Oceanography. 2009; 22: 160–171. https://doi.org/10.5670/oceanog.2009.105

8. Garcia HE, Cosca C, Kozyr A, Mayorga E, Chandler C, Thomas RW, et al. Data management strategy to improve global use of ocean acidification data and information. Oceanography. 2015; 28: 226–228. https://doi.org/10.5670/oceanog.2015.45

9. McLaughlin K, Weisberg SB, Dickson AG, Hofmann GE, Newton JA, Aseltine-Neilson D, et al. Core principles of the california current acidification network: Linking chemistry, physics, and ecological effects. Oceanography. 2015; 28: 160–169. https://doi.org/10.5670/oceanog.2015.39

10. Millero FJ. Chemical Oceanography, Third Edition. CRC Press. Taylor & Francis; 2006. Available: https://books.google.com.br/books?id=Xt5T8LtPjBgC

11. Millero FJ. Carbonate constants for estuarine waters. Mar Freshw Res. 2010; 61: 139. https://doi.org/10.1071/MF09254

12. Orr JC, Epitalon J-M, Dickson AG, Gattuso J-P. Routine uncertainty propagation for the marine carbon dioxide system. Mar Chem. 2018; 207: 84–107. https://doi.org/10.1016/j.marchem.2018.10.006

13. Ramos e Silva CA, De Miranda LB, Dávalos PB, Da Silva MP. Hydrochemistry in tropical hyper-saline and positive estuaries. Panam J Aquat Sci. 2010; 5: 432–443.

14. Ramos e Silva CA, Sternberg L da SL, Dávalos PB, Souza FES de. The impact of organic and intensive farming on the tropical estuary. Ocean Coast Manag. 2017; 141: 55–64. https://doi.org/10.1016/j.ocecoaman.2017.03.010

15. Ramos e Silva CA, Senez-Mello TM, Fonseca EM da, Ribeiro HM, Neto JAB, Damasceno RN. Acidificação dos oceanos em um sopro: Prática educacional para construção de conhecimento das mudanças globais. Rev Experiências em Ensino Ciências. 2017; 12: 1–25.

16. Reid JL. On the total geostrophic circulation of the South Atlantic Ocean: Flow patterns, tracers, and transports. Prog Oceanogr. 1989; 23: 149–244. https://doi.org/10.1016/0079-6611(89)90001-3

17. Stramma L, Peterson RG. The South Atlantic Current. J Phys Oceanogr. 1990; 20: 846–859. https://doi.org/10.1175/1520-0485(1990)020<0846:TSAC>2.0.CO;2

18. Tsuchiya M. Circulation of the Antarctic Intermediate Water in the North Atlantic Ocean. J Mar Res. 2004; 47: 747–755. https://doi.org/10.1357/002224089785076136

19. Silva AC da, Araújo M, Bourlès B. Variação sazonal da estrutura de massas de água na plataforma continental do Amazonas e área oceânica adjacente. Rev Bras Geofísica. 2005; 23: 145–157. https://doi.org/10.1590/S0102-261X2005000200004

20. Silveira ICA Da. O Sistema Corrente do Brasil na Bacia de Campos, RJ. Thesis, Instituto Oceanográfico, Universidade de São Paulo. Universidade de São Paulo. 2007.

21. Moreira DL, Carneiro MER, Silva AP, Schwamborn R. Caracterização Ambiental da Bacia de Sergipe e sul de Alagoas. In: Carneiro MER, editor. Ambiente Pelágico da Bacia de Sergipe—Alagoas Coleção Projeto Marseal, livro 3. 2019. p. 579.

22. Campos EJD, Velhote D, da Silveira ICA. Shelf break upwelling driven by Brazil Current Cyclonic Meanders. Geophys Res Lett. 2000; 27: 751–754. https://doi.org/10.1029/1999GL010502

23. Bates NR. Seawater Carbonate Chemistry Distributions Across the Eastern South Pacific Ocean Sampled as Part of the GEOTRACES Project and Changes in Marine Carbonate Chemistry Over the Past 20 Years. Front Mar Sci. 2018; 5: 1–18. https://doi.org/10.3389/fmars.2018.00398

24. Perretti AR, de Albergaria-Barbosa ACR, Kerr R, da Cunha LC. Ocean acidification studies and the uncertainties relevance on measurements of marine carbonate system properties. Brazilian Journal of Oceanography. 2018. https://doi.org/10.1590/s1679-87592018000706602

25. Luiz Augusto Bizzi, Schobbenhaus C, Vidotti RM, Gonçalves JH. Geologia, tectônica e recursos minerais do Brasil: texto, mapas & SIG. CPRM–Serviço Geológico do Brasi. Brasília: CPRM—Companhia de Pesquisa de Recursos Minerais; 2003.

26. Knoppers B, Ekau W, Figueiredo AG. The coast and shelf of east and northeast Brazil and material transport. Geo-Marine Letters. 1999. pp. 171–178. https://doi.org/10.1007/s003670050106

27. INMET CDP. Boletim Agroclimatológico Mensal De Maio—2014. Inst Nac Desenvolv e Pesqui. 2014; 48: 42. Available: http://www.inmet.gov.br/portal/arq/upload/BOLETIM-AGRO_MENSAL_201405.pdf

28. DOE. Handbook of methods for the analysis of the various parameters of the carbon dioxide system in sea water; version 2. ORNL/CDIAC-74. Oak Ridge, TN; 1994. https://doi.org/10.2172/10107773

29. Ramos e Silva CA, Liu X, Millero FJ. Solubility of siderite ($FeCO_3$) in NaCl solutions. J Solution Chem. 2002; 31: 97–108. https://doi.org/10.1023/A:1015275618138

30. Wolf-Gladrow DA, Zeebe RE, Klaas C, Körtzinger A, Dickson AG. Total alkalinity: The explicit conservative expression and its application to biogeochemical processes. Mar Chem. 2007; 106: 287–300. https://doi.org/10.1016/j.marchem.2007.01.006

31. Marion GM, Millero FJ, Camões MF, Spitzer P, Feistel R, Chen C-TA. pH of seawater. Mar Chem. 2011; 126: 89–96. https://doi.org/10.1016/j.marchem.2011.04.002

32. Pratt KW. Measurement of pHT values of Tris buffers in artificial seawater at varying mole ratios of Tris: Tris·HCl. Mar Chem. 2014; 162: 89–95. https://doi.org/10.1016/j.marchem.2014.03.003

33. Tomczak M. A multi-parameter extension of temperature/salinity diagram techniques for the analysis of non-isopycnal mixing. Prog Oceanogr. 1981; 10: 147–171. https://doi.org/10.1016/0079-6611(81)90010-0

34. Tomczak M, Tanner E. An estimate of bass strait water movement in the western tasman sea during the australian coastal experiment. Mar Freshw Res. 1989. https://doi.org/10.1071/MF9890465

35. McDougall, Trevor J, Barker PM. Getting started with TEOS-10 and the Gibbs Seawater (GSW) Oceanographic Toolbox. Scor/Iapso Wg127. 2011; 28. SCOR/IAPSO WG127

36. Van Den Berg CMG, Rogers H. Determination of alkalinities of estuarine waters by a two-point potentiometric titration. Mar Chem. 1987; 20: 219–226. https://doi.org/10.1016/0304-4203(87)90073-9

37. Dickson AG. Thermodynamics of the dissociation of boric acid in synthetic seawater from 273.15 to 318.15 K. Deep Sea Res Part A Oceanogr Res Pap. 1990; 37: 755–766. https://doi.org/10.1016/0198-0149(90)90004-F

38. Hunter KA. The temperature dependence of pH in surface seawater. Deep Res Part I Oceanogr Res Pap. 1998. https://doi.org/10.1016/S0967-0637(98)00047-8

39. Perez FF, Fraga F. The pH measurements in seawater on the NBS scale. Mar Chem. 1987. https://doi.org/10.1016/0304-4203(87)90054-5

40. Millero FJ, Zhang JZ, Fiol S, Sotolongo S, Roy RN, Lee K, et al. The use of buffers to measure the pH of seawater. Mar Chem. 1993. https://doi.org/10.1016/0304-4203(93)90199-X

41. Clayton TD, Byrne RH. Spectrophotometric seawater pH measurements: total hydrogen ion concentration scale calibration of m-cresol purple and at-sea results. Deep Res Part I. 1993. https://doi.org/10.1016/0967-0637(93)90048-8

42. Millero FJ. The pH of estuarine waters. Limnol Oceanogr. 1986; 31: 839–847. https://doi.org/10.4319/lo.1986.31.4.0839

43. Millero FJ. Thermodynamics of the carbon dioxide system in the oceans. Science. 1995; 59: 661–677.

44. Millero F rank J. Chemical Oceanography, Second Edition. CRC Press. Taylor & Francis; 1996. Available: https://books.google.com.br/books?id=KhqYHXfcT0gC

45. Millero FJ. The physical chemistry of natural waters. Pure Appl Chem. 1985; 57: 1015–1024. https://doi.org/10.1351/pac198557081015

46. Lueker TJ, Dickson AG, Keeling CD. Ocean pCO_2 calculated from dissolved inorganic carbon, alkalinity, and equations for K_1 and K_2: Validation based on laboratory measurements of CO_2 in gas and seawater at equilibrium. Mar Chem. 2000; 70: 105–119. https://doi.org/10.1016/S0304-4203(00)00022-0

47. Yao W, Millero FJ. The chemistry of the anoxic waters in the Framvaren Fjord, Norway. Aquat Geochemistry. 1995; 1: 53–88. https://doi.org/10.1007/BF01025231

48. Roy RN, Roy LN, Vogel KM, Porter-Moore C, Pearson T, Good CE, et al. The dissociation constants of carbonic acid in seawater at salinities 5 to 45 and temperatures 0 to 45˚C. Mar Chem. 1993; 44: 249–267. https://doi.org/10.1016/0304-4203(93)90207-5

49. Millero FJ, Graham TB, Huang F, Bustos-Serrano H, Pierrot D. Dissociation constants of carbonic acid in seawater as a function of salinity and temperature. Mar Chem. 2006; 100: 80–94. https://doi.org/10.1016/j.marchem.2005.12.001

50. Silveira ICA da. Massas de água e circulação do talude continental e região oceânica da Bacia de Sergipe- Alagoas. Oceanogr e Meteorol. 2015; 4.

51. Emílsson I. The shelf and coastal waters off southern Brazil. Bol do Inst Ocean. 1961; 11: 101–112. https://doi.org/10.1590/s0373-55241961000100004

52. Stramma L, Schott F. The mean flow field of the tropical Atlantic Ocean. Deep Res Part II Top Stud Oceanogr. 1999; 46: 279–303. https://doi.org/10.1016/S0967-0645(98)00109-X

53. Silveira ICA Da Schmidt ACK, Campos EJD Godoi SS De, Ikeda Y. A corrente do Brasil ao largo da costa leste brasileira. Brazilian J Oceanogr. 2000; 48: 171–183. https://doi.org/10.1590/S1679-87592000000200008

54. Sverdrup HU, Murphy RC, Johnson MW, Fleming RH. The Oceans: Their Physics, Chemistry, and General Biology. Geogr Rev. 1944. https://doi.org/10.2307/210609

55. Dickson AG, Sabine CL, Christian JR. Guide to best practices for ocean CO_2 measurements. PICES Spec Publ 3. 2007; 3: 191. https://doi.org/10.1159/000331784

56. Uppström L. The boron/Chlorinity ratio of deep-sea water from the Pacific Ocean. Deep-Sea Research. 1974; 21: 161–162.

57. Kulinski K, Szymczycha B, Koziorowska K, Hammer K, Schneider B. Anomaly of total boron concentration in the brackish waters of the Baltic Sea and its consequence for the CO_2 system calculations. Marine Chemistry. 2018, 11–19. https://doi.org/10.1016/j.marchem.2018.05.007

58. Millero FJ, Lee K, Roche M. Distribution of alkalinity in the surface waters of the major oceans. Marine Chemistry. 1998. https://doi.org/10.1016/S0304-4203(97)00084-4

59. Egleston ES, Sabine CL, Morel FMM. Revelle revisited: Buffer factors that quantify the response of ocean chemistry to changes in DIC and alkalinity. Global Biogeochem Cycles. 2010; 24: 1–9. https://doi.org/10.1029/2008GB003407

60. Jiang ZP, Tyrrell T, Hydes DJ, Dai M, Hartman SE. Variability of alkalinity and the alkalinity-salinity relationship in the tropical and subtropical surface ocean. Global Biogeochem Cycles. 2014. https://doi.org/10.1002/2013GB004678

61. Chester R. Marine Geochemistry. Liverpool: Academic Division of Unwin Hyman Ltd; 1990. https://doi.org/10.1007/978-94-010-9488-7

62. Feely RA, Sabine CL, Hernandez-Ayon JM, Ianson D, Hales B. Evidence for Upwelling of Corrosive "Acidified" Water onto the Continental Shelf. Science. 2008; 320: 1490–1492. https://doi.org/10.1126/science.1155676 PMID: 18497259

63. Takahashi T. The Fate of Industrial Carbon Dioxide. Science. 2004; 305: 352–353. https://doi.org/10.1126/science.1100602

64. Smith HEK, Tyrrell T, Charalampopoulou A, Dumousseaud C, Legge OJ, Birchenough S, et al. Predominance of heavily calcified coccolithophores at low $CaCO_3$ saturation during winter in the Bay of Biscay. Proc Natl Acad Sci U S A. 2012; 109: 8845–8849. https://doi.org/10.1073/pnas.1117508109 PMID: 22615387

65. Kleypas JA. Impacts of ocean acidification on marine biodiversity. Biodiversity and Climate Change: Transforming the Biosphere. 2019. pp. 185–195. https://doi.org/10.2307/j.ctv8jnzw1.25

66. Kleypas JA, Yates KK. Coral reefs and ocean acidification. Oceanography. 2009; 22: 108–117. https://doi.org/10.5670/oceanog.2009.101

67. Taylor AR, Brownlee C, Wheeler GL. Proton channels in algae: Reasons to be excited. Trends in Plant Science. Elsevier Ltd; 2012. pp. 675–684. https://doi.org/10.1016/j.tplants.2012.06.009 PMID: 22819465

68. Allemand D, Tambutté É, Zoccola D, Tambutté S. Coral Calcification, Cells to Reefs. Coral Reefs: An Ecosystem in Transition. Dordrecht: Springer Netherlands; 2011. pp. 119–150. https://doi.org/10.1007/978-94-007-0114-4_9

69. Hurd CL, Beardall J, Comeau S, Cornwall CE, Havenhand JN, Munday PL, et al. Ocean acidification as a multiple driver: how interactions between changing seawater carbonate parameters affect marine life. Mar Freshw Res. 2019; 71: 263. https://doi.org/10.1071/MF19267

70. Fassbender AJ, Sabine CL, Feifel KM. Consideration of coastal carbonate chemistry in understanding biological calcification. Geophys Res Lett. 2016. https://doi.org/10.1002/2016GL068860

71. Waldbusser GG, Hales B, Haley BA. Calcium carbonate saturation state: On myths and this or that stories. ICES Journal of Marine Science. 2016. https://doi.org/10.1093/icesjms/fsv174

72. Bockmon EE, Dickson AG. An inter-laboratory comparison assessing the quality of seawater carbon dioxide measurements. Mar Chem. 2015; 171: 36–43. https://doi.org/10.1016/j.marchem.2015.02.002